JOURNAL OF Materials Communication CHEMISTRY

# Influence of drying technique on silicon insertion into γ-alumina and consequences for the homogeneity and thermal stability of silica–alumina aquagels

**Aurelian F. Popa,† Sylvie Rossignol and Charles Kappenstein***

*Laboratoire de Catalyse par les Métaux, Equipe de Chimie Minérale, LACCO UMR 6503, Université de Poitiers, 40 avenue du Recteur Pineau, F-86022 Poitiers cedex, France. E-mail: Charles.Kappenstein@univ-poitiers.fr*

***Received 29th May 2002, Accepted 30th July 2002***
***First published as an Advance Article on the web 8th August 2002***

**Si-doped alumina gels of nominal composition $(Al_2O_3)_{0.88}$–$(SiO_2)_{0.12}$ have been synthesised in aqueous media and dried under different conditions in order to obtain xerogel (drying at 120 °C) or aerogel (supercritical $CO_2$ drying) forms; after heating at 1200 °C for 5 h, the aerogel samples are more homogenous and retain a better specific surface area (>100 $m^2$ $g^{-1}$) than the xerogel samples.**

High thermal stability is required for alumina supports in applications like high temperature catalytic combustion of hydrocarbons,[1] methane steam reforming[2] or catalytic decomposition of monopropellant for space applications.[3] The key to preserving a good surface area is to suppress or delay the ultimate transformation into the thermodynamically stable α-alumina phase (corundum). Possible ways of attaining this goal are decreasing of the bulk density of transition aluminas by supercritical drying[4] or addition of small quantities of doping elements like Ba, Mg and La.[5] A literature survey showed that interesting results have been obtained by combining these two procedures, in order to prepare Si-doped alumina aerogels in supercritical ethanol,[6–10] but no work focussing on a comparison between the structure and properties of xerogels and aerogels. We present here preliminary results on this comparison.

We have prepared samples of nominal composition $(Al_2O_3)_{0.88}$–$(SiO_2)_{0.12}$ (Si : Al atomic ratio 6 : 94) according to the Yoldas procedure,[11] under excess water ($H_2O$ : Al molar ratio 100 : 1). The synthesis was carried out using $Al(O^{sec}C_4H_9)_3$ as a molecular precursor. After 1 h at 60 °C, the corresponding amount of $Si(OC_2H_5)_4$ was slowly added, followed by a small quantity of HCl (Al+Si : HCl = 1 : 0.07). The mixture was heated to 80 °C and maintained at that temperature for 2 h in a covered beaker in order to avoid solvent evaporation. Then, the beaker was left open to the atmosphere for several hours at the same temperature and gelling occurred. After gelling and cooling, the sample was dried at 120 °C for 12 h in an oven, leading to the xerogel form.

In order to prepare the aerogel form, the water inside a second gel sample was quantitatively exchanged for acetone over 5 to 6 days by adding fresh acetone twice a day. Then, supercritical $CO_2$ drying was carried out in a 300 ml autoclave (Parr Instruments), at about 40 °C and 140 bar over 2 h.

Both xerogel and aerogel samples were then calcined for 5 h at 1200 °C in air. X-Ray diffraction measurements (XRD) were carried out on a θ–θ Siemens D5005 apparatus, using Cu radiation, in the 2θ range 20–90°. The BET surface area was determined by nitrogen adsorption on a Micromeritics ASAP 2000 device. Scanning transmission electron microscopy and energy dispersive X-ray emission (EDX) analysis were performed using a Philips CM 120 microscope.

The XRD profiles of both dried gels exhibit the structural features of hydrated pseudo-boehmite $AlO(OH)\cdot nH_2O$,[12] with a specific surface area of more than 300 $m^2$ $g^{-1}$. After the thermal treatment, the aerogel sample has a specific surface area of 103 $m^2$ $g^{-1}$, whereas the corresponding value for the xerogel form was 67 $m^2$ $g^{-1}$; the surface area of the aerogel is similar to that found by Mizushima and Hori (114 $m^2$ $g^{-1}$)[13,14] for a 10% doped sample prepared in an alcoholic medium. Both samples correspond to the θ-alumina phase. It should be noted that for pure alumina in xerogel or aerogel forms, the same heating conditions lead to collapse of the structure and complete transformation into the α-alumina phase (specific surface area in the range 1 to 3 $m^2$ $g^{-1}$).

Careful examination of the diffraction patterns of the calcined samples shows a slight but always detectable systematic shift of the aerogel peak positions toward higher 2θ values with respect to those of the xerogel (Fig. 1). This displacement can be explained by cell parameter shrinkage due to the presence of silicon atoms in the tetrahedral sites of the transition alumina structure; silicon atoms are slightly smaller than aluminium atoms (Si–O bond length = 1.60 Å, whereas Al–O = 1.76 Å). Nevertheless, the precise positions of these peaks are difficult to establish because of superposition of the X-ray lines characteristic of the θ-alumina structure. Since this structure can be viewed as a distorted spinel structure,[15] we can approximate the peak displacement on the basis of a cubic structure; assuming that all the silicon atoms are inserted into the tetrahedral sites of the alumina structure, we can estimate the calculated 2θ displacement at between 0.2 and 0.5°. The experimental shifts between the aerogel and the xerogel peak

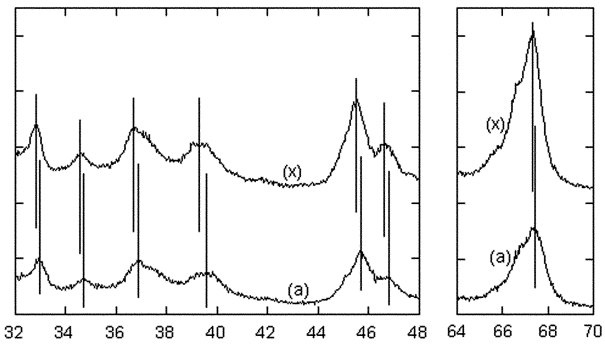


**Fig. 1** X-Ray diffractograms for $(Al_2O_3)_{0.88}$–$(SiO_2)_{0.12}$ samples: (a) = aerogel, (x) = xerogel.

†Current address: University "Al. I. Cuza", b-dul Carol I, nr.11, Lasi 6600, Romania.

 DOI: 10.1039/b205209c

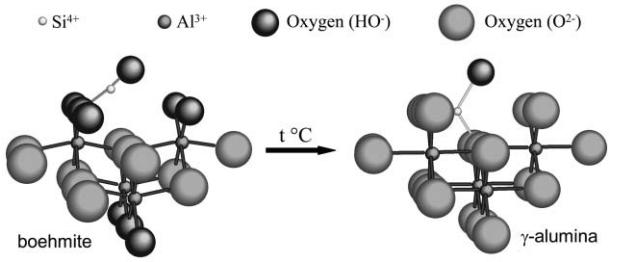


**Fig. 2** Possible scheme for silicon insertion into the γ-alumina structure during the boehmite transformation.

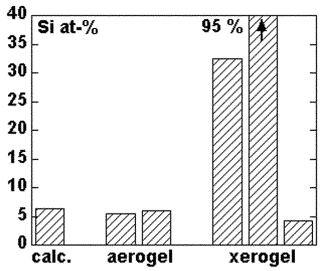


**Fig. 4** Silicon atom percentage from EDX analysis for $(Al_2O_3)_{0.88}$–$(SiO_2)_{0.12}$ aerogel and xerogel samples.

positions range from 0.1 to 0.3°, proving that the silicon percentage inserted into the alumina structure is higher in the case of the aerogel (of the order of 50%).

This cell parameter difference is not found for the non-calcined samples displaying the boehmite structure; the diffractograms revealed no displacement between the peaks of both samples, in agreement with the boehmite structure which displays only octahedral sites able to host aluminium atoms but not silicon. During the sol synthesis, boehmite nanocrystallites are formed by hydrolysis of the aluminium precursor. After addition of the silicon precursor, the hydrolysis leads to silicon species which can bond to surface aluminium atoms by $\mu_2$-oxo bridges, as a consequence of oxolation reactions (eqn. 1).

$$\text{–Si–OH} + \text{HO–Al–} \rightarrow \text{–Si–O–Al–} + H_2O \qquad (1)$$

Before calcination, the silicon atoms remain mainly on the surface of the boehmite crystallites and they can migrate into the bulk only during the transformation into γ-alumina (Fig. 2). The presence of these silicon atoms stabilises the alumina defect structure and could explain the delay of the transformation into corundum.

Fig. 3 shows typical transmission electron microscopy results, including Al and Si mappings for both samples. The most striking difference is the more homogeneous repartition of Al and Si for the aerogel sample. The xerogel sample shows the presence of heterogeneous areas containing more silicon, in agreement with the TEM pictures. Typical EDX spectra are also reported (Fig. 3) showing areas with higher silicon concentration for the xerogel sample. Typical values of the atomic silicon percentage {*i.e.* [Si/(Si + Al)] × 100} are given in Fig. 4. For the aerogel sample, these values are in agreement with the calculated value (6.4 at%), whereas the data are much more divergent for the xerogel sample; values much higher than the calculated value in small areas and even nearly pure amorphous silicon particles are visible (Fig. 3 and 4). To compensate for the presence of these silica-rich particles, the majority of the surface displays silicon percentages less than the calculated value with a more homogeneous dispersion. In contrast, for the aerogel, no silica particles could be identified. The silica segregation in the case of the xerogel explains the difference in the specific surface areas between the samples.

In conclusion, the drying technique exerts a major influence on the morphological properties of silica–alumina mixed materials; this could explain the different thermal stability of the xerogel and aerogel samples and bring about more interest in such materials for high temperature applications. One question that remains open is the fate of the silicon atoms during the heating stage: (i) formation of silica crystallites by migration of individual Si atoms from the surface of boehmite crystallites in the case of the xerogel or (ii) insertion into the tetrahedral sites of the defect spinel lattice of transition alumina for the aerogel form, as shown in Fig. 2. The first option is favoured by the densification of the gel during the drying process. After the drying stage, the silicon atoms cover the small pseudo-boehmite crystallites. For the dense xerogel, the closeness of the crystallites facilitates the formation of silica or silica-rich particles during the transformation of pseudo-boehmite into transition aluminas. On the other hand this process seems to be more difficult in the case of the aerogel, due to the greater initial separation length between the primary particles, and therefore facilitates the incorporation of some of the silicon atoms into the structure of the transition alumina. The alumina particles are consequently better stabilised in the aerogel sample.

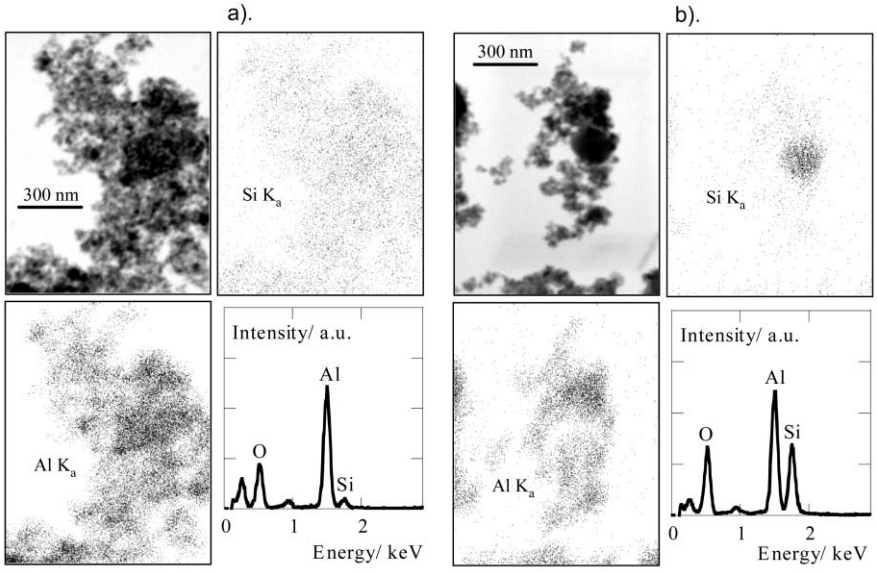


**Fig. 3** TEM micrographs, typical silicon and aluminium mappings, and EDX analyses for $(Al_2O_3)_{0.88}$–$(SiO_2)_{0.12}$ for (a) aerogel and (b) xerogel samples.

## Acknowledgements

The authors thank E. Gautron for the microscopy and EDX analysis. A. F. P. thanks the French Government for a doctoral co-channel grant, and Prof. G. Pajonck for a practical stay.

## Notes and references

1 D. L. Trimm, H. Arai and H. Fukuzawa, *Catal. Today*, 1995, **26**, 217.
2 K. Kochloefl, in *Handbook of Heterogeneous Catalysis*, ed. G. Ertl, H. Knözinger and J. Weitkamp, Wiley-VCH,, Weinheim, Germany, 1997, p. 1819.
3 E. Schmidt, *Hydrazine and its Derivatives. Preparation, Properties, Applications*, J. Wiley, New York, 2nd edn. 2001, p. 1268.
4 T. Horiuchi, T. Osaki, T. Sugiyama, H. Masuda, M. Horio, K. Suzuki, T. Mori and S. T. Toshiaki, *J. Chem. Soc., Faraday. Trans.*, 1994, **90**, 2573.
5 S. Rossignol and C. Kappenstein, *Int. J. Inorg. Mater.*, 2001, **3**, 51.
6 T. Horiuchi, L. Chen, T. Osaki, T. Sugiyama, K. Suzuki and T. Mori, *Catal. Lett.*, 1999, **58**, 89.
7 T. Horiuchi, T. Osaki, T. Sugiyama, K. Suzuki and T. Mori, *J. Non-Cryst. Solids*, 2001, **291**, 187.
8 C. Hernandez and A. C. Pierre, *Langmuir*, 2000, **16**, 530.
9 Z. Novak, Z. Knez, V. Kaucic and N. N. Tusar, *Chem. Tech. (Leipzig)*, 1999, **51**, 191.
10 J. B. Miller and E. I. Ko, *Catal. Today*, 1998, **43**, 51.
11 B. E. Yoldas, *J. Mater. Sci.*, 1975, **10**, 1856.
12 R. Tettenhorst and D. A. Hofmann, *Clays Clay Miner.*, 1980, **28**, 373.
13 Y. Mizushima and M. Hori, *J. Mater. Res.*, 1993, **8**(11), 2993.
14 Y. Mizushima and M. Hori, *J. Non-Cryst. Solids*, 1994, **167**, 1.
15 R. S. Zhou and R. L. Snyder, *Acta. Crystallogr., Sect. B*, 1991, **47**, 617.